

Pygmy and giant dipole resonances in Ni isotopesJun Liang,^{1,2,*} Li-Gang Cao,¹ and Zhong-Yu Ma^{1,3,†}¹*China Institute of Atomic Energy, Beijing 102413, People's Republic of China*²*Department of Physics, Taiyuan University of Technology, Taiyuan 030024, People's Republic of China*³*Center of Theoretical Nuclear Physics, National Laboratory of Heavy Ion Accelerator of Lanzhou, Lanzhou 730000, People's Republic of China*

(Received 19 December 2006; published 17 May 2007)

The isovector giant and pygmy dipole resonances in even-even Ni isotopes are studied within the framework of a fully consistent relativistic random-phase approximation built on the relativistic mean field ground state. An additional isoscalar-isovector nonlinear coupling term is adopted in the standard effective mean field Lagrangian, which could modify the density dependence of the symmetry energy and soften the symmetry energy at the saturation density without changing the agreement with experimentally existing data of ground state properties. We found that the centroid energy of the isovector giant dipole resonance is tightly correlated to the neutron skin thickness. In contrast, the centroid energy of the isovector pygmy resonance is insensitive to the density dependence of the symmetry energy by tuning the isoscalar-isovector nonlinear coupling.

DOI: [10.1103/PhysRevC.75.054320](https://doi.org/10.1103/PhysRevC.75.054320)

PACS number(s): 21.60.Jz, 24.30.Cz, 24.10.Jv, 27.50.+e

I. INTRODUCTION

Since the isovector electric (non-spin-flip) giant dipole resonance (GDR) was investigated first by Bandwin and Klailer [1] at the end of 1940s, the experimental and theoretical investigation of various modes of nuclear collective excitations has become a major research field in nuclear structure physics. Especially, much experimental data on GDR have been obtained [2–4]. In recent years, the investigation of the new low-energy collective isovector dipole mode, i.e., isovector pygmy dipole resonance (PDR), has attracted much experimental and theoretical attention. The onset of low-lying E_1 strength has been observed not only in exotic nuclei with a large neutron excess but also in stable nuclei [5–8]. PDR is a result of excess neutrons oscillating out of phase with a core composed of an equal number of protons and neutrons, which is different from GDR, which represents a coherent oscillation of all protons against all neutrons and is the quintessential nuclear mode; a large fraction of the energy-weighted sum rule is exhausted by this one resonance. Although the strength of PDR is small compared to the total dipole strength, it is a very important mode of nuclear excitation. The occurrence of PDR significantly enhances the radiative neutron capture cross section on neutron-rich nuclei [9,10], which has significance in astrophysics. On the other hand, many theoretical works have been carried out to understand the nature of both GDR and PDR [11–16].

According to macroscopic hydrodynamic models, the restoring force of isovector GDR is proportional to the symmetry energy of nuclear matter. The symmetry energy plays an important role in understanding the mechanisms of many exotic phenomena in nuclear physics and astrophysics. It affects directly the properties of exotic nuclei, dynamics of heavy ion collisions, structure of neutron stars, simulation

of supernova core collapse, and so on. Unfortunately, our knowledge of symmetry energy is rather poor, especially regarding its density dependence. Correlations between the basic properties of the mean field models and symmetry energy parameters with the size of the neutron skin have been studied in Ref. [17]. There is no sufficient resolution in the binding energy systematics of finite nuclei to fix the symmetry energy. Additional isovector observables, such as binding energies of more asymmetric nuclei, and observables from collective excitations will be needed [17]. A systematic investigation of GDR and PDR and correlations between GDR, PDR, and the symmetry energy may provide valuable information on the density dependence of the symmetry energy.

In this work, a fully consistent relativistic random-phase approximation (RRPA) built on the relativistic mean field (RMF) ground state [18–20] is applied in studying GDR and PDR in Ni isotopes. An additional isoscalar-isovector nonlinear coupling is introduced in the RMF effective Lagrangian, which could soften the symmetry energy and keep the ground state properties in good agreement with the experimental data. Varying the strengths of the isoscalar-isovector nonlinear coupling modifies the density dependence of the symmetry energy as well as the neutron skin. Alternatively, one could explicitly include density-dependent meson-nucleon coupling constants to soften the density dependence of the symmetry energy [21]. We will include the isoscalar-isovector nonlinear coupling term in the RMF + RRPA calculations and systematically investigate the correlation of GDR, PDR, density dependence of symmetry energy, and neutron skin thickness in Ni isotopes.

The manuscript has been organized as follows. In Sec. II, the ground state properties of Ni isotopes are studied in the RMF theory with an additional nonlinear coupling of isoscalar and isovector mesons. A fully consistent RRPA built on the RMF ground state is briefly presented in Sec. III. In Sec. IV, GDR and PDR in even-even Ni isotopes are discussed. Finally, a brief summary is given in Sec. V.

*Electronic address: liangjun@ciae.ac.cn†Electronic address: mazy12@ciae.ac.cn

II. GROUND STATE PROPERTIES OF Ni ISOTOPES IN THE RELATIVISTIC MEAN FIELD THEORY

We start with an effective Lagrangian of the form

$$\begin{aligned} \mathcal{L} = & \bar{\psi} [\gamma^\mu (i\partial_\mu - g_\omega \omega_\mu - g_\rho \mathbf{f}\tau \cdot \mathbf{b}_\mu - \frac{1}{2}e(1 + \tau_3)A_\mu) \\ & - (M + g_\sigma \sigma)] \psi + \frac{1}{2} \partial^\mu \sigma \partial_\mu \sigma - \frac{1}{2} m_\sigma^2 \sigma^2 - \frac{1}{4} \omega^{\mu\nu} \omega_{\mu\nu} \\ & + \frac{1}{2} m_\omega^2 \omega^\mu \omega_\mu - \frac{1}{4} \mathbf{B}^{\mu\nu} \cdot \mathbf{B}_{\mu\nu} + \frac{1}{2} m_\rho^2 \mathbf{b}^\mu \cdot \mathbf{b}_\mu \\ & - \frac{1}{4} F^{\mu\nu} F_{\mu\nu} - U_{\text{eff}}(\sigma, \omega^\mu, \mathbf{b}^\mu), \end{aligned} \quad (1)$$

where $M, m_\sigma, m_\omega, m_\rho$ are the nucleon, σ, ω , and ρ masses, respectively, while $g_\sigma, g_\omega, g_\rho$, and $e^2/4\pi = 1/137$ are the corresponding coupling constants for mesons and the photon. Various field tensors have been defined as

$$\omega_{\mu\nu} = \partial_\mu \omega_\nu - \partial_\nu \omega_\mu, \quad (2)$$

$$\mathbf{B}_{\mu\nu} = \partial_\mu \mathbf{b}_\nu - \partial_\nu \mathbf{b}_\mu, \quad (3)$$

$$F_{\mu\nu} = \partial_\mu A_\nu - \partial_\nu A_\mu, \quad (4)$$

$$U_{\text{eff}}(\sigma, \omega^\mu) = \frac{1}{3} g_2 \sigma^3 + \frac{1}{4} g_3 \sigma^4 - \frac{1}{4} c_3 (\omega^\mu \omega_\mu)^2, \quad (5)$$

where g_2, g_3 , and c_3 are the nonlinear coupling parameters for self-interactions of the scalar and vector fields. In addition, a mixed nonlinear isoscalar-isovector coupling with a strength Λ_v is introduced, that is,

$$U_{\text{eff}}(\omega^\mu, \mathbf{b}^\mu) = -4\Lambda_v g_\rho^2 \mathbf{b}_\mu \cdot \mathbf{b}^\mu g_\omega^2 \omega_\mu \omega^\mu, \quad (6)$$

which could soften the density dependence of the symmetry energy. This softening occurs by tuning the nonlinear coupling strength Λ_v . With increasing Λ_v , the symmetry energy becomes weaker at the saturation density and stronger at lower densities (see Fig. 1 and Table I).

Although the symmetry energy at saturation density is not well constrained experimentally, some average of that energy and of the surface energy may be constrained by binding energies [17,24]. As a simple approximation, we keep the symmetry energy fixed at the average density $\rho = 0.1 \text{ fm}^{-3}$, which is at the nuclear surface. This simple prescription produces a nearly constant proton radius and binding energy, only the neutron radius and neutron skin thickness S , which is a quantity defined as the difference between the root-mean-square (rms) radii of neutrons and protons, $\sqrt{\langle r_n^2 \rangle} - \sqrt{\langle r_p^2 \rangle}$, are changed. The ground state properties of Ni isotopes ($A = 64-78$) are calculated in the RMF with the parameter sets NL3 [22] and TM1 [23]. The neutron skin thickness S is reduced with the additional mixed nonlinear isoscalar-isovector coupling, while the binding energy per nucleon and the proton radius remain unchanged (see Figs. 2 and 3).

TABLE I. Saturation density and symmetry energy at saturation density.

Model	Λ_v	$a_{\text{sym}}^{\text{sat}}$ (MeV)	ρ_{sat} (fm^{-3})
NL3	0.0	37.4	0.148
	0.025	32.4	
TM1	0.0	36.9	0.145
	0.030	32.1	

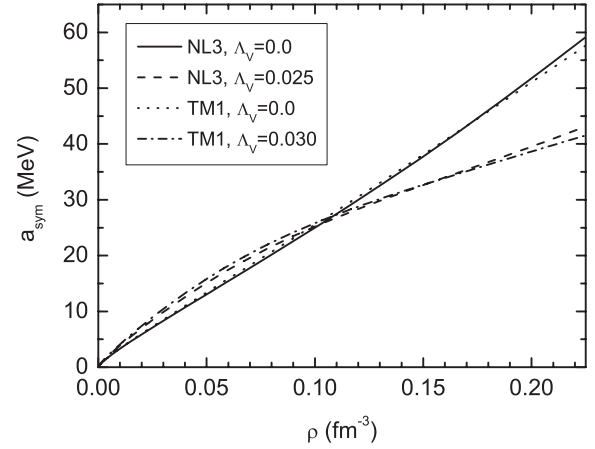


FIG. 1. Density dependence of symmetry energy in nuclear matter for NL3 [22] and TM1 [23] parameter sets.

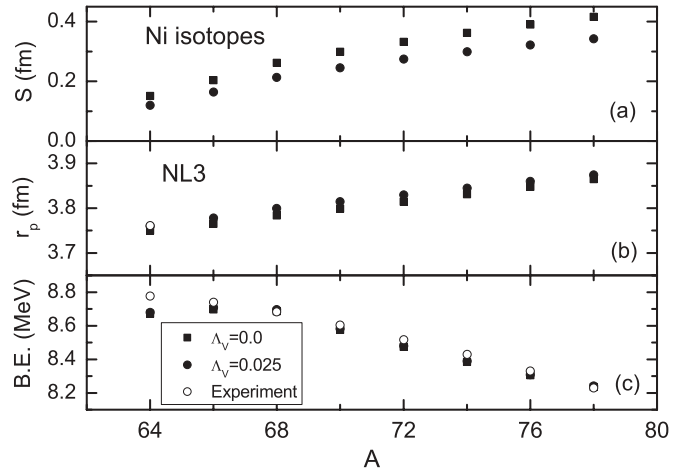


FIG. 2. Calculated (a) neutron skin thickness S , (b) proton radius, and (c) binding energy per nucleon for even-even Ni isotopes; all calculations were performed with parameter set NL3. Experimental data, when available, are from Refs. [25,26].

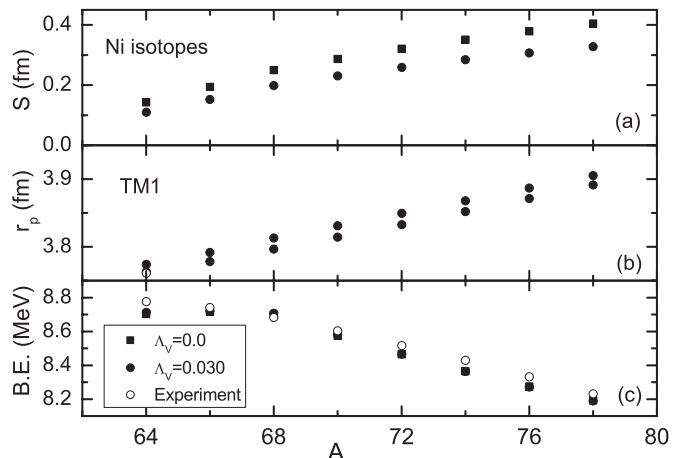


FIG. 3. Same as Fig. 2, but for parameter set TM1.

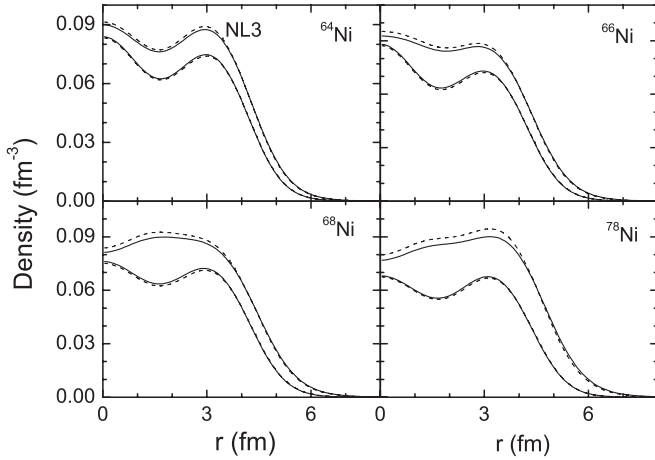


FIG. 4. Neutron and proton density distributions in Ni isotopes in the RMF with NL3 for two different values of the nonlinear ω - ρ coupling. Cases $\Lambda_v = 0$ and $\Lambda_v = 0.025$ are denoted by solid and dash curves, respectively. Lower and upper curves in each panel are proton and neutron density distributions, respectively.

The proton and neutron density distributions of isotopes ^{64}Ni , ^{66}Ni , ^{68}Ni , and ^{78}Ni are plotted in Fig. 4. They are calculated with and without the mixed nonlinear isoscalar-isovector coupling in the RMF with NL3. In the calculation, both pairing correlations and the coupling to more complex configurations are neglected.

The solid and dashed curves correspond to the results for $\Lambda_v = 0$ and $\Lambda_v = 0.025$, respectively. Clearly, the neutron central neutron densities with the softening of the symmetry energy, while the proton densities essentially remain unchanged. Therefore, the neutron skin S becomes smaller as Λ_v increases. And the larger the neutron number N , the more prominent is the increase of the neutron central density. This suggests that the bigger the neutron number N , the larger the change of the neutron skin thickness S , which is shown in Figs. 2 and 3.

III. FULLY CONSISTENT RELATIVISTIC RANDOM-PHASE APPROXIMATION

The fully consistent RRPA is built on the RMF ground state. Details of the RRPA method used in the present study are described in Refs. [18–20]. The linear response of a system to an external field is given by the imaginary part of the retarded polarization operator

$$R(Q, Q; \mathbf{k}, \mathbf{k}', E) = \frac{1}{\pi} \text{Im} \Pi(Q, Q; \mathbf{k}, \mathbf{k}'; E), \quad (7)$$

where Q is a one-body operator represented by a 4×4 matrix. $Q = \gamma^0 r Y_{10} \tau$ for dipole resonance, which excites an ($L = 1$)-type electric (non-spin-flip) ($\Delta T = 1$ and $\Delta S = 0$) giant resonance with spin and parity $J^\pi = 1^-$. The retarded polarization operator Π can be obtained by solving the

Bethe-Salpeter equation [27]

$$\begin{aligned} \Pi(Q, Q; \mathbf{k}, \mathbf{k}', E) = & \Pi_0(Q, Q; \mathbf{k}, \mathbf{k}', E) \\ & - \sum_i g_i^2 \int d^3 k_1 d^3 k_2 \Pi_0(Q, \Gamma^i; \\ & \times \mathbf{k}, \mathbf{k}_1, E) D_i(\mathbf{k}_1 - \mathbf{k}_2, E) \Pi \\ & \times (\Gamma_i, Q; \mathbf{k}_2, \mathbf{k}', E), \end{aligned} \quad (8)$$

where Π_0 is the unperturbed (Hartree) polarization operator. The residual particle-hole interactions are generated by the meson exchanges, described by corresponding propagators D_i . In this equation, the index i runs over σ , ω , and ρ mesons with g_i being the corresponding coupling constants. Because of the nonlinear couplings, the effective meson propagators $D_i(\mathbf{k}_1 - \mathbf{k}_2, E)$ cannot be obtained analytically. In field theory, equations of motion for fermion and boson fields are obtained by variations of the action with respect to the corresponding fields. The first-order variation of the action with respect to a given meson field ϕ gives the field equation (Klein-Gordon equation) satisfied by this field. The second-order variation of the action at the classical value ϕ_0 of the meson field ϕ will lead to the equation of the meson propagator [28]

$$\left(\partial^\mu \partial_\mu + \frac{\partial^2 U_{\text{eff}}(\phi)}{\partial \phi^2} \Big|_{\phi_0} \right) D_\phi(x, y) = -\delta^4(x, y). \quad (9)$$

In practice, it is more convenient to calculate $D_\phi(x, y)$ by solving the above equation in the momentum space [19]. Taking the Fourier transform of Eq. (9), we obtain the expression of the meson propagator in the momentum space

$$\begin{aligned} (E^2 - \mathbf{k}^2) D_\phi(\mathbf{k}, \mathbf{k}', E) - \frac{1}{2\pi^3} \\ \times \int S_\phi(\mathbf{k} - \mathbf{k}_1) D_\phi(\mathbf{k}, \mathbf{k}', E) d^3 k_1 = (2\pi)^3 \delta(\mathbf{k} - \mathbf{k}'), \end{aligned} \quad (10)$$

where $S_\phi(\mathbf{k} - \mathbf{k}_1)$ is the Fourier transform of $\frac{\partial^2 U_\phi(\phi)}{\partial \phi^2} \Big|_{\phi_0}$,

$$S_\phi(\mathbf{k} - \mathbf{k}_1) = \int e^{-i(\mathbf{k} - \mathbf{k}_1) \cdot \mathbf{r}} V_\phi d^3 r. \quad (11)$$

Therefore, the function V_ϕ for σ , ω , and ρ mesons can be expressed, respectively, as

$$V_\sigma = m_\sigma^2 + 2g_2 \sigma(r) + 3g_3 \sigma^2(r), \quad (12)$$

$$V_\omega = m_\omega^2 + 3c_3 \omega_0^2(r) + 8\Lambda_v g_\rho^2 g_\omega^2 b_0^2(r), \quad (13)$$

$$V_\rho = m_\rho^2 + 8\Lambda_v g_\rho^2 g_\omega^2 \omega_0^2(r). \quad (14)$$

$\sigma(r)$, $\omega_0(r)$, and $b_0(r)$ are the classical values of σ , ω , and ρ fields. They can be obtained by a self-consistent calculation in the RMF [28].

IV. GIANT AND PYGMY DIPOLE RESONANCES

The giant dipole resonances in the Ni isotopes are calculated with parameter sets NL3 and TM1. A spherical symmetry is adopted to simplify the RRPA calculations, where the density distributions for nucleons in an open shell are averaged (filling approximation) [14]. To obtain the centroid energies of dipole

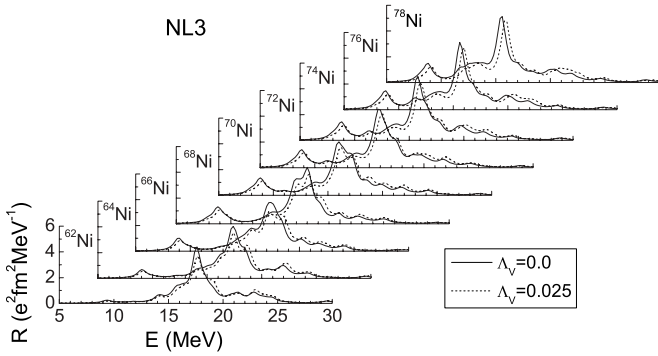


FIG. 5. Isovector dipole response functions in Ni isotopes, for parameter set NL3 with two different values of the nonlinear ω - ρ coupling. Cases with $\Lambda_v = 0$ and $\Lambda_v = 0.025$ are denoted by solid and dash curves, respectively.

resonance strengths, we first calculate various moments of the response function in a given interval, that is,

$$m_k = \int_0^{E_{\max}} R^L(E) E^k dE. \quad (15)$$

E_{\max} is the maximum excitation energy, which is carried out to 60 MeV in the present calculations. To study PDR, the centroid energies are calculated separately in two energy regions: 0–10 and 10–60 MeV. From those moments, we can obtain the centroid energies of PDR and GDR, $\bar{E} = m_1/m_0$.

We display the distribution of isovector dipole strength for the even-even Ni isotopes in Figs. 5 and 6 with the parameter sets NL3 and TM1, respectively. In Fig. 5, the GDR peak is around 17 MeV and that of PDR is around 9 MeV. The PDR strengths increase as the neutron number increases. The results with parameter set TM1 are very similar.

To show the correlation between the symmetry energy, neutron skin, and evolution of GDR and PDR in Ni isotopes, we plot the centroid energies of GDR and PDR as functions of nuclear mass and neutron skin in Figs. 7–10. In Figs. 7 and 9 we compare the centroid energies of GDR for Ni isotopes with (solid circles) and without (solid squares) the isoscalar-isovector coupling, where the parameter sets NL3 and TM1 are used. It is found in Figs. 7 and 9 that with increasing Λ_v and decreasing neutron skin thickness, the centroid energy of GDR increases for all Ni isotopes. It is well known that the restoring force of the isovector

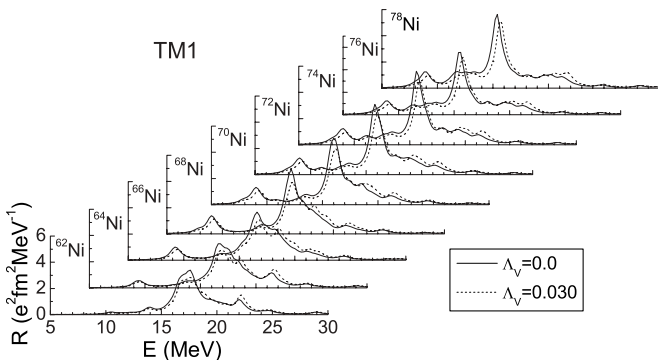


FIG. 6. Same as Fig. 5, but for parameter set TM1.

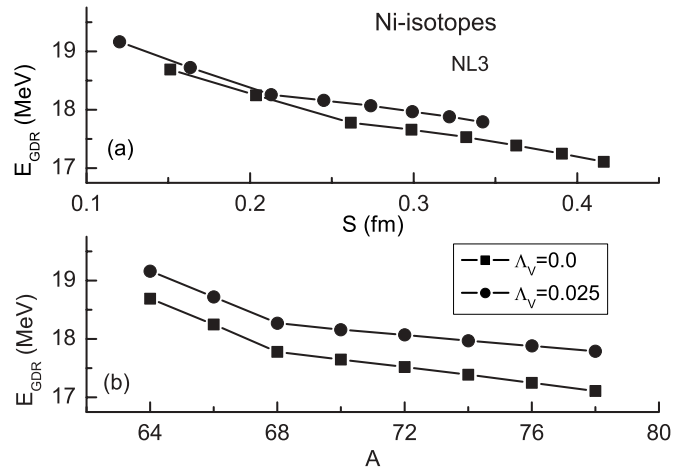


FIG. 7. Centroid energy of GDR as functions of (a) neutron skin thickness S and (b) mass number of the Ni isotopes, for parameter set NL3.

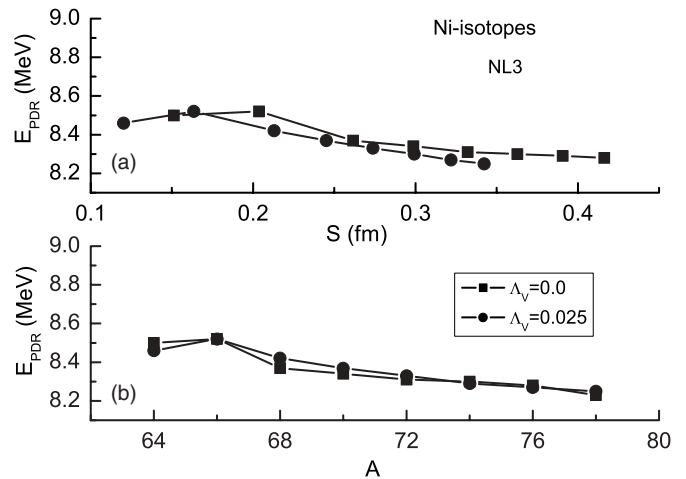


FIG. 8. Same as Fig. 7, but for PDR.

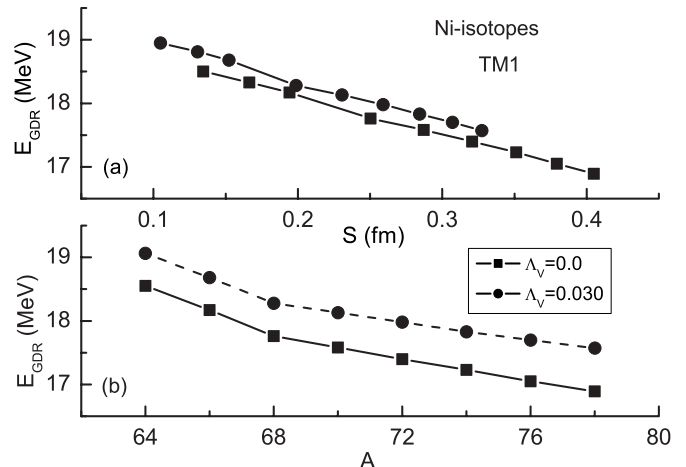


FIG. 9. Same as Fig. 7, but for parameter set TM1.

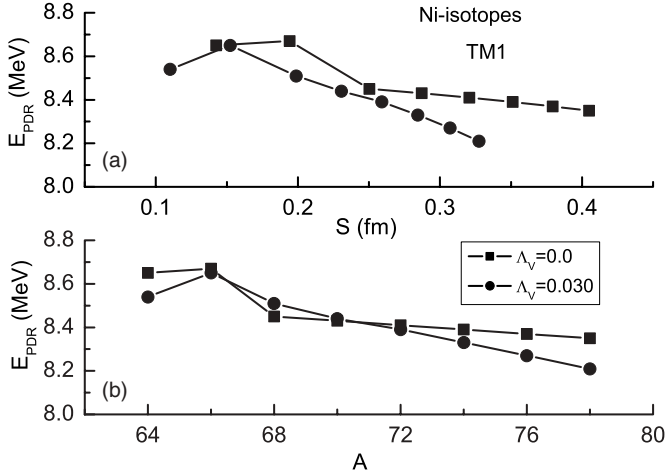


FIG. 10. Same as Fig. 8, but for parameter set TM1.

GDR is proportional to the volume symmetry energy. It has been mentioned above that with increasing Λ_v , the symmetry energy becomes soft. Although the symmetry energy decreases at saturation density, the symmetry energy becomes stronger at lower densities below $\rho = 0.1 \text{ fm}^{-3}$ (see Fig. 1). Due to the surface vibration modes of the collective excitations, the centroid energies of GDR are pushed to higher energies with stronger symmetry energy at low density. And as the number of neutrons increases, the isospin effect becomes stronger. For each isotope, the neutron skin is reduced with softening of the symmetry energy. Because we plotted the centroid energy of GDR as a function of neutron skin, a tight correlation is clearly shown between the centroid energy of the GDR state and the neutron skin thickness in the Ni isotopes [Figs. 7(a) and 9(a)].

In contrast, it is interesting to find in Figs. 8 and 10 that the centroid energies of the PDR are insensitive to any change in the density dependence of the symmetry energy caused by tuning Λ_v . Similar results have been observed in studies of nuclei ^{130}Sn and ^{132}Sn [13]. These results show that the isoscalar-isovector nonlinear coupling has no effect on the PDR centroids. The reason is because the PDR originates mainly from the vibrations of a few valence neutrons against the nuclear core. Those valence neutrons are located at the density, where the symmetry energy is not changed. Actually, in Fig. 4 one can observe that the neutron density distributions in both cases for the isoscalar-isovector coupling constants are basically the same in the exterior region which is relevant to the dynamics of PDR. The main difference is observed in the interior region, which has very little influence on the subtle properties of PDR. To achieve variations in the neutron skin which are relevant to PDR, one needs to obtain modified neutron density distributions at larger radii, and exactly this is achieved in Ni isotopes by increasing the number of neutrons, which is shown in Figs. 8(a) and 10(a).

We close the discussion by displaying in Fig. 11 the calculated fraction of the energy-weighted sum rule contained in PDR relative to that in GDR with parameter set TM1 as a function of the mass number A for Ni isotopes. Obviously, a strong linear correlation between $m_1(\text{PDR})/m_1(\text{GDR})$ and A is displayed for $A \leq 68$. With increasing mass number A , the neutron skin increases, which support the point of view that

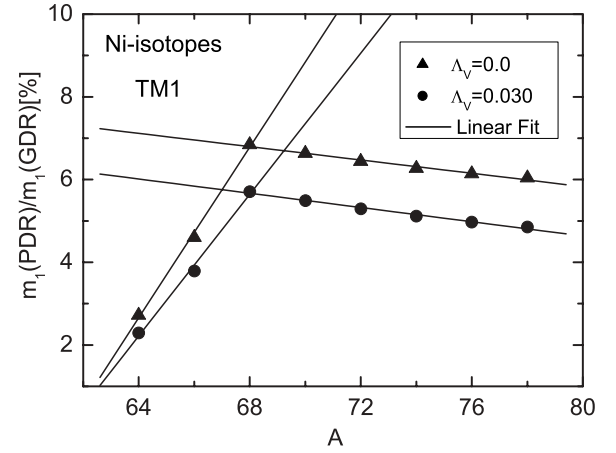


FIG. 11. Fraction of energy-weighted sum rule contained in PDR relative to that in GDR as a function of the mass number A for Ni isotopes, for parameter set TM1.

the PDR is considered to be an oscillation of the neutron skin against the isospin symmetric core. The mild anticorrelation in the evolution from ^{68}Ni to ^{78}Ni can be attributed to the neutron orbital $1g_{9/2}$. This high-angular-momentum orbital plays a passive role in driving the low-energy transition of low multipolarity [13]. In addition, there is a noticeable decrease in the fraction of the energy-weighted sum rule contained in PDR relative to that in GDR with increasing Λ_v , i.e., decreasing neutron skin. This result is consistent with that obtained in ^{130}Sn and ^{132}Sn [13].

V. SUMMARY

In summary, the isovector giant dipole and pygmy resonances in even-even Ni isotopes are studied within the framework of a fully consistent relativistic random-phase approximation built on effective mean field ground state. The effective Lagrangians with additional isoscalar-isovector nonlinear coupling term is introduced. The isoscalar-isovector nonlinear coupling term could soften the symmetry energy in nuclear matter and, therefore, the neutron skin thickness in finite nuclei. The effects of the isoscalar-isovector nonlinear coupling term on the isovector dipole response including the centroid energies of GDR and PDR and the relative transition strength of PDR with respect to GDR in Ni isotopes were investigated. We found that the centroid energy of the isovector giant dipole resonance is tightly correlative to the neutron skin thickness. In contrast, the centroid energy of the isovector pygmy resonance is insensitive to the changing of the density dependence of the symmetry energy by tuning Λ_v .

ACKNOWLEDGMENTS

This work is supported by the National Natural Science Foundation of China under Grant Nos. 10475116, 10535010, 10235020 and by the Asia-Europe Link in Nuclear Physics and Astrophysics CN/ASIA-LINK/008 (094-791).

- [1] B. C. Baldwin and G. S. Klailer, *Phys. Rev.* **71**, 3 (1947).
- [2] B. L. Berman and S. C. Fultz, *Rev. Mod. Phys.* **47**, 713 (1975).
- [3] J. Speth, *Electric and Magnetic Giant Resonances in Nuclei* (World Scientific, Singapore, 1991.)
- [4] J. Ritman *et al.*, *Phys. Rev. Lett.* **70**, 533 (1993).
- [5] T. Aumann *et al.*, *Nucl. Phys.* **A649**, 297c (1999).
- [6] N. Ryezayeva *et al.*, *Phys. Rev. Lett.* **89**, 272502 (2002).
- [7] J. Enders *et al.*, *Nucl. Phys.* **A724**, 243 (2003).
- [8] T. Hartmann, M. Babilon, S. Kamedzhiev, E. Litvinova, D. Savran, S. Volz, and A. Zilges, *Phys. Rev. Lett.* **93**, 192501 (2004).
- [9] S. Goriely and E. Khan, *Nucl. Phys.* **A706**, 217 (2002).
- [10] S. Goriely, E. Khan, and M. Samyn, *Nucl. Phys.* **A739**, 331 (2004).
- [11] D. Vretenar, N. Paar, P. Ring, and G. A. Lalazissis, *Nucl. Phys.* **A692**, 496 (2001).
- [12] N. Paar, D. Vretenar, and P. Ring, *Phys. Rev. Lett.* **94**, 182501 (2005).
- [13] J. Piekarewicz, *Phys. Rev. C* **73**, 044325 (2006).
- [14] Z. Y. Ma, H. Toki, B. Q. Chen, and N. V. Giai, *Prog. Theor. Phys.* **98**, 917 (1997).
- [15] D. Vretenar, N. Paar, P. Ring, and G. A. Lalazissis, *Phys. Rev. C* **63**, 047301 (2001).
- [16] N. Paar, T. Niksic, D. Vretenar, and P. Ring, *Phys. Lett.* **B606**, 288 (2005).
- [17] R. J. Furnstahl, *Nucl. Phys.* **A706**, 85 (2002).
- [18] Z. Y. Ma, N. V. Giai, A. Wandelt, D. Vretenar, and P. Ring, *Nucl. Phys.* **A686**, 173 (2001).
- [19] Z. Ma, N. Van Giai, H. Toki, and M. L'Huillier, *Phys. Rev. C* **55**, 2385 (1997).
- [20] N. V. Giai, Z. Y. Ma, H. Toki, and B. Q. Chen, *Nucl. Phys.* **A649**, 37c (1999).
- [21] D. Vretenar, T. Niksic, and P. Ring, *Phys. Rev. C* **68**, 024310 (2003).
- [22] G. A. Lalazissis, J. König, and P. Ring, *Phys. Rev. C* **55**, 540 (1997).
- [23] Y. Sugahara and H. Toki, *Nucl. Phys.* **A579**, 557 (1994).
- [24] B. A. Brown, *Phys. Rev. Lett.* **85**, 5296 (2000).
- [25] H. De Vries, C. W. De Jager, and C. De Vries, *At. Data Nucl. Data Tables* **36**, 495 (1987).
- [26] G. Audi, A. H. Wapstra, and C. Thibault, *Nucl. Phys.* **A729**, 337 (2003).
- [27] A. L. Fetter and J. D. Walecka, *Quantum Theory of Many-Particle Systems* (McGraw-Hill, New York, 1977).
- [28] B. D. Serot and J. D. Walecka, *Adv. Nucl. Phys.* **16**, 1 (1986).